Electrochemistry and the Dependence of Potentials on pH of Iron and Manganese Tetraphenylporphyrins in Aqueous Solution

Thomas W. Kaaret, Guo-Hua Zhang, and Thomas C. Bruice*

Contribution from the Department of Chemistry, University of California at Santa Barbara, Santa Barbara, California 93106. *Received September 7, 1990*

Abstract: Microelectrode electrochemical studies have been carried out with aqueous solutions (μ = 0.2 with $NaNO_3$) of the water soluble and non-μ-oxo dimer forming 5,10,15,20-tetrakis(2,6-dimethyl-3-sulfonatophenyl)porphinatoiron(III) and -manganese(III) hydrates [(**1**)$Fe^{III}(X_2)$ and (**1**)$Mn^{III}(X)_2$, X = H_2O, HO^-, and O^{2-}]. The pH dependence of the potentials (SCE) for the stepwise 1e$^-$ oxidations of (**1**$^{\bullet-}$)$Fe^{II}(X)_2 \rightarrow$ (**1**)$Fe^{II}(X)_2 \rightarrow$ (**1**)$Fe^{III}(X)_2 \rightarrow$ (**1**)$Fe^{IV}(X)_2 \rightarrow$ (**1**$^{\bullet+}$)$Fe^{IV}(X)_2$ and (**1**)$Mn^{III}(X)_2 \rightarrow$ (**1**)$Mn^{IV}(X)_2 \rightarrow$ (**1**)$Mn^{V}(X)_2$ were determined from Nernst-Clark plots of E_m values (determined at constant pH) vs pH. Also obtained from the Nernst-Clark plots are the pK_a values for the acid dissociation of the water molecules ligated to [(**1**)Fe^{III}]$^+$, [(**1**)Fe^{IV}]$^{2+}$, [(**1**$^{\bullet+}$)Fe^{IV}]$^{3+}$ and to [(**1**)Mn^{III}]$^+$, [(**1**)Mn^{IV}]$^{2+}$, and [(**1**)Mn^{V}]$^{3+}$. The midpoint potentials for the 1e$^-$ oxidations (**1**$^{\bullet-}$)$Fe^{II}(X)_2 \rightarrow$ (**1**)$Fe^{II}(X)_2$ and (**1**)$Fe^{IV}(X)_2 \rightarrow$ (**1**$^{\bullet+}$)$Fe^{IV}(X)_2$ are pH independent, due to the equality of the pK_a values of water ligated to reduced and oxidized species, and equal -1.15 and 1.17 V (SCE), respectively. Representative values of $E^{\circ\prime}$ for the interconversion of the various iron(III) and iron(IV) porphyrin hydrates are e$^-$ + (**1**)$Fe^{IV}(H_2O)_2 \rightarrow$ (**1**)$Fe^{III}(H_2O)_2$, 0.91 V; e$^-$ + (**1**)$Fe^{IV}(H_2O)(OH) \rightarrow$ (**1**)$Fe^{III}(H_2O)(OH)$, 0.86 V; and e$^-$ + (**1**)$Fe^{IV}(OH)_2 \rightarrow$ (**1**)$Fe^{III}(OH)_2$, 0.77 V. The best first and second pK_a values at μ = 0.2 for the dissociation of protons from the ligated water molecules are (**1**$^{\bullet-}$)$Fe^{II}(H_2O)_2$ and (**1**)$Fe^{II}(H_2O)_2$, pK_{a1} 9.7; (**1**)$Fe^{III}(H_2O)_2$, pK_{a1} 6.55 and pK_{a2} 10.55; (**1**)$Fe^{IV}(H_2O)_2$ and (**1**$^{\bullet+}$)$Fe^{IV}(H_2O)_2$, pK_{a1} 5.7 and pK_{a2} 9.0. Spectroelectrochemical studies of the controlled potential oxidation of (**1**)$Fe^{III}(X)_2 \rightarrow$ (**1**)$Fe^{IV}(X)_2$ show that the various iron(IV) species, formed at different pH values, possess the same spectral characteristics as seen previously in the 1e$^-$ oxidation of (**1**)$Fe^{III}(X)_2$ by *tert*-butyl hydroperoxide in water. Comparison of plots of E_m vs pH in H_2O to E_m vs pD plots in D_2O for the oxidation of (**1**)$Fe^{III}(X)_2 \rightarrow$ (**1**)$Fe^{IV}(X)_2$ shows that there is no (within experimental error) deuterium isotope effects upon potentials. The deuterium isotope effects upon the acidity of ligated $H(D)_2O$ (K_a^H/K_a^D) are (L = H or D) (**1**)$Fe^{III}(L_2O)_2 \rightarrow$ (**1**)$Fe^{III}(LO)(L_2O)$ + L^+, 5.0; (**1**)$Fe^{III}(LO)(L_2O) \rightarrow$ (**1**)$Fe^{III}(LO)_2$ + L^+, 2.8; (**1**)$Fe^{IV}(L_2O)_2 \rightarrow$ (**1**)-$Fe^{IV}(LO)(L_2O)$ + L^+, 7.9; (**1**)$Fe^{IV}(LO)(L_2O) \rightarrow$ (**1**)$Fe^{IV}(LO)_2$ + L^+, 3.55. Representative values of $E^{\circ\prime}$ for the interconversion of the various manganese(III) and manganese(IV) porphyrin hydrates are e$^-$ + (**1**)$Mn^{IV}(H_2O)_2 \rightarrow$ (**1**)$Mn^{III}(H_2O)_2$, 1.04 V; e$^-$ + (**1**)$Mn^{IV}(H_2O)(OH) \rightarrow$ (**1**)$Mn^{III}(H_2O)(OH)$, 0.93 V; e$^-$ + (**1**)$Mn^{IV}(HO)_2 \rightarrow$ (**1**)$Mn^{III}(HO)_2$, 0.79 V. First and second pK_a values for the dissociation of manganese ligated water are (**1**)$Mn^{III}(H_2O)_2$, pK_{a1} 5.8 and pK_{a2} 12.2; (**1**)$Mn^{IV}(H_2O)_2$, pK_{a1} 4.1 and pK_{a2} 9.9; and for (**1**)$Mn^{V}(H_2O)_2$, pK_{a1} 3.7. Our thermodynamic data (both E_m and pK_a values) supports an iron(IV) porphyrin π-cation radical [(**1**$^{\bullet+}$)$Fe^{IV}(X)_2$] rather than an iron(V) porphyrin [(**1**)$Fe^{V}(X)_2$] as the product of 2e$^-$ oxidation of (**1**)$Fe^{III}(X)_2$. On the other hand, our data support a manganese(V) porphyrin [(**1**)$Mn^{V}(X)_2$] rather than a manganese(IV) porphyrin π-cation radical. Of considerable importance is the finding, in water, that H_2O and HO^- serve as the axial ligands for [(porph)M]$^{2+}$ and [(porph)M]$^{3+}$ species and that oxo ligation [as in (**1**$^{\bullet+}$)Fe^{IV}(=O)] cannot be important except at high pH [where structures as (**1**$^{\bullet+}$)$Fe^{IV}(OH)_2$ and (**1**$^{\bullet+}$)Fe^{IV}(=O)(H_2O) have the same proton inventory].

Introduction

As judged by the number of recent publications, there is much interest in the mechanisms of oxidation of metal(III) porphyrins to yield higher valent metal-oxo porphyrins[1] and the reactions of the latter with organic substrates.[2] In order to understand these processes it is useful to have a knowledge of the solvent and acidity dependence of the potentials E_1 and E_2 of eq 1 (where X = H_2O, HO^-, or O^{2-}). In an oxidation reaction the change in

$$\{(\text{porph}^{\bullet+})M^{IV}(X) \text{ or } (\text{porph})M^{V}(X)\} + e^- \rightleftharpoons (\text{porph})M^{IV}(X)\ E_1$$

$$(\text{porph})M^{IV}(X) + e^- \rightleftharpoons (\text{porph})M^{III}(X)\ E_2 \qquad (1)$$

standard free energy ($\Delta\Delta G^\circ$) for the formation of products (or intermediates) on transfer of a reaction from one solvent to another is determined by the solvent dependence of the redox potentials of oxidant and substrate. Reactions which involve reactants or intermediates with ionizable protons and/or processes which involve proton transfer are best studied (when possible) in aqueous solutions where acidity and ionic strength are easily controlled. The values of the potentials E_1 and E_2 are dependent upon the nature of the axial ligands. In water solvent, in the presence of weakly ligating bases, the axial ligands are represented by HO^- or H_2O depending upon the pH. Studies in water have the advantage that one can determine the dependence of the log of the rate constant (k) upon pH. From log k vs pH rate profiles and a knowledge of the ionization constants of reactants, one can identify the reacting species at various acidities. From the dependence of potential on pH (i) acid ionization constants of reactants may be determined, (ii) choices may be made between kinetically equivalent mechanisms, and (iii) the magnitude of the rate constants for reactions occurring in different pH regions may be explained.

We report here an investigation of the dependence of the various oxidation and reduction potentials for the water soluble and non-μ-oxo dimer forming 5,10,15,20-tetrakis(2,6-dimethyl-3-sulfonatophenyl)porphinatoiron(III) and -manganese(III) hydrates [(**1**)$Fe^{III}(X)_2$ and (**1**)$Mn^{III}(X)_2$, X = H_2O, HO^-, and O^{2-}].

Experimental Section

Materials. Preparation of 5,10,15,20-Tetrakis(2,6-dimethyl-3-sulfonatophenyl)porphinatoiron(III) and -manganese(III) Hydroxides {(1)$Fe^{III}(OH)(H_2O)$ and (1)$Mn^{III}(OH)(H_2O)$}. 5,10,15,20-Tetrakis-(2,6-dimethylphenyl)porphine [(Me_8TPP)H_2] was prepared by the me-

(1) (a) Balasubramanian, P. N.; Lee, R. W.; Bruice, T. C. *J. Am. Chem. Soc.* **1989**, *111*, 8714. (b) Bruice, T. C.; Balasubramanian, P. N.; Lee, R. W.; Smith. J. R. L. *J. Am. Chem. Soc.* **1988**, *110*, 7890. (c) Smith, J. R. L.; Balasubramanian, P. N.; Bruice, T. C. *J. Am. Chem. Soc.* **1988**, *110*, 7411. (d) Lee, W. A.; Yuan, L.-C.; Bruice, T. C. *J. Am. Chem. Soc.* **1988**, *110*, 4277. (e) Arasasingham, R. D.; Cornman, C. R.; Balch, A. L. *J. Am. Chem. Soc.* **1989**, *111*, 7800. (f) Arasasingham, R. D.; Balch, A. L.; Cornman, C. R.; Latos-Grazynski, L. J. *J. Am. Chem. Soc.* **1989**, *111*, 4357. (g) Arasasingham, R. D.; Balch, A. L.; Latos-Grazynski, L. J. *J. Am. Chem. Soc.* **1987**, *109*, 5846. (h) Traylor, T. G.; Ciccone, J. P. *J. Am. Chem. Soc.* **1989**, *111*, 8413.

(2) (a) Ostovic, D.; Bruice, T. C. *J. Am. Chem. Soc.* **1989**, *111*, 6511. (b) Garrison, J. M.; Ostovic, D.; Bruice, T. C. *J. Am. Chem. Soc.* **1989**, *111*, 4960. (c) Lee, R. W.; Nakagaki, P. C.; Bruice, T. C. *J. Am. Chem. Soc.* **1989**, *111*, 1368. (d) Castellino, A. J.; Bruice, T. C. *J. Am. Chem. Soc.* **1988**, *111*, 1313. (e) Ostovic, D.; Bruice, T. C. *J. Am. Chem. Soc.* **1988**, *111*, 6906. (f) Castellino, A. J.; Bruice, T. C. *J. Am. Chem. Soc.* **1988**, *111*, 752. (g) Hickman, D. L.; Nanthakumar, A.; Goff, H. M. *J. Am. Chem. Soc.* **1988**, *111*, 6384. (h) Traylor, T. G.; Xu, F. *J. Am. Chem. Soc.* **1988**, *111*, 1953. (i) Groves, J. T.; Stern, M. K. *J. Am. Chem. Soc.* **1988**, *111*, 8628.

0002-7863/91/1513-4652$02.50/0

thod of Lindsay.[3] The 2,6-dimethylbenzaldehyde starting material was prepared by refluxing a solution composed of 15 g (0.10 mol) of 2,6-dimethylbenzaldehyde oxime (Aldrich), 20 g (0.13 mol) of *p*-nitrobenzaldehyde, 90 mL of concentrated HCl, and 365 mL of distilled-deionized water for 2 h. After cooling to room temperature, the reaction mixture was extracted with ether (3 × 100 mL). Ether fractions were combined and extracted with 0.5 N NaOH (3 × 100 mL), to remove *p*-nitrobenzaldehyde oxime, until the aqueous layer was only slightly yellow. The ether fraction was then washed with water (3 × 100 mL) and brine and then dried with $MgSO_4$. Rotatory evaporation gave a yellow oil which was taken up in a minimal volume of hot $CHCl_3$ followed by flash chromatography (SiO_2 250–400 mesh; ethyl acetate/hexane (10/90)). The 2,6-dimethylbenzaldehyde fractions were collected, and after evaporation there was obtained 11 g of product. Kugelrhor distillation gave 7.1 g (0.05 mol) of 2,6-dimethylbenzaldehyde (52%) (R_f 0.8 using SiO_2 TLC; ethyl acetate/hexane (15/85)).

[(**1**)H_2] was prepared by the sulfonation of $(Me_8TPP)H_2$ by using the method of Zipplies et al.[4] Water-soluble metalloporphyrins (**1**)Fe^{III}(O-H)(H_2O) and (**1**)Mn^{III}(OH)(H_2O) were then prepared by refluxing [(**1**)H_2] and a 50-fold excess of the metal(II)-acetate in salt in water between a pH of 6–8 for a period of 7–24 hours. The water-soluble metalloporphyrins were purified by ultrafiltration and ion-exchange and size-exclusion chromatographies. Characterization of (**1**)Fe^{III}(O-H)(H_2O) and (**1**)Mn^{III}(OH)(H_2O) by NMR, UV-visible, IR, and elemental analysis agree with previously reported values.[4,5]

Electrochemical Measurements. All aqueous solutions used for electrochemistry were prepared from distilled-deionized water which was boiled at least 0.5 h and stored under argon scrubbed free of O_2, CO, and CO_2. Samples in D_2O were prepared in a similar manner from 99.9 atom % deuterium oxide (Aldrich). Preparations of all solutions were carried out under a nitrogen atmosphere scrubbed free of O_2, CO, and CO_2. Metalloporphyrin concentrations ranged from 0.8 to 5.2 mM in aqueous 0.2 N $NaNO_3$. Dilute solutions of carbonate-free HNO_3 and NaOH were used for the adjustment of pH.

The following buffers were employed in spectroelectrochemical experiments: (pH 3.1) $ClCH_2COO^-/ClCH_2COOH$, (pH 5.2) CH_3COO^-/CH_3COOH, (pH 6.7 and 7.2) $H_2PO_3^-/HPO_3^{2-}$, (pH 9.3) HCO_3^-/CO_3^{2-}, (pH 10.6) HO^-/H_2O. Ionic strength was maintained at 0.2 with $NaNO_3$. Controlled potential electrolysis, in each buffer, was carried out at a potential 0.100 V greater than the midpoint potential as measured by cyclic voltammetry at a carbon fiber microelectrode.

Instrumentation. The potentiostats used were a Princeton Applied Research Model 174 (Princeton, NJ), a Bioanalytical Systems Model CV-27 Voltograph (West Lafayette, IN), or a Cypress Systems Model CYSY-1 Computer-Controlled Electrolysis System (Lawrence, KS). A Pine Instrument Co. ASR rotator was used in rotating disk experiments. A Pt flag electrode separated from the analyte compartment by a medium porosity frit was used as the auxiliary electrode. An Ag/AgCl electrode standardized to 0.00 V vs SCE was used as the reference electrode.

A carbon microelectrode (7-μm diameter) was employed as the working electrode for the determination of the pH dependence of potentials in aqueous solution. The carbon microelectrodes were constructed by using a previously described procedure.[6,7] Magnamite graphite fibers were obtained from Hercules (Magna, UT). Epon resin 828 was obtained from Shell Oil Co. (Houston, TX). *m*-Phenylenediamine was obtained from Eastman Organic Chemicals (Rochester, NY). The glassy carbon electrode used for rotating disk experiments was 0.765 cm in diameter. A Pt mesh working electrode was used in spectroelectrochemical experiments. The design of the spectroelectrochemical cells employed have been described.[8,9]

Data Handling. Nernst–Clark plots of potential vs pH were computer fitted as previously described[10] by a computer program obtained from Professor Edward Skibo, Arizona State University, Department of Chemistry.

(3) Lindsay, J. S.; Schreiman, I. C.; Hsu, H. C.; Kearney, P. C.; Marguerettaz, A. M. *J. Org. Chem.* **1987**, *52*, 827.
(4) Zipplies, M. F.; Lee, W. A.; Bruice, T. C. *J. Am. Chem. Soc.* **1986**, *108*, 4433.
(5) Balasubramanian, P. N.; Schmidt, E. S.; Bruice, T. C. *J. Am. Chem. Soc.* **1987**, *109*, 7865.
(6) Dayton, M. A.; Brown, J. C.; Stutts, K. J.; Wightman, R. M. *Anal. Chem.* **1980**, *52*, 946.
(7) Fleischmann, M.; Pons, S.; Rolison, D. R.; Schmidt, P. P. *Ultramicroelectrodes*; Datatech Systems, Inc.: Morganton, NC, 1987; pp 65–90.
(8) (a) Lin, X. Q.; Kadish, K. M. *Anal. Chem.* **1985**, *57*, 1498. (b) Lin, X. Q.; Kadish, K. M. *Anal. Chem.* **1986**, *58*, 1493.
(9) Calderwood, T. S.; Lee, W. A.; Bruice, T. C. *J. Am. Chem. Soc.* **1985**, *107*, 8272.
(10) Eberlein, G.; Bruice, T. C. *J. Am. Chem. Soc.* **1983**, *105*, 6685.

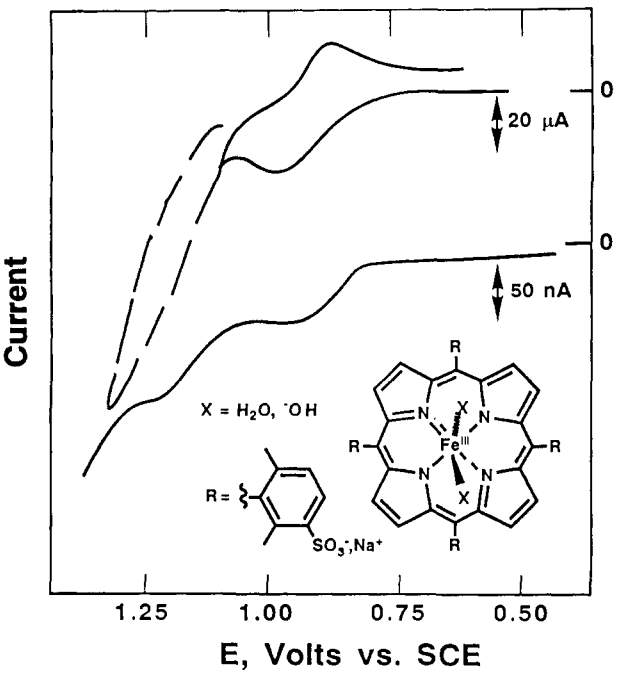

Figure 1. Structure and 0.20 V/s voltammograms of 3.1 mM (**1**)Fe^{III}-$(X)_2$ in aqueous acetate buffer at pH 5.2: bottom, 7-μm carbon microelectrode and top, 1-mm glassy carbon electrode.

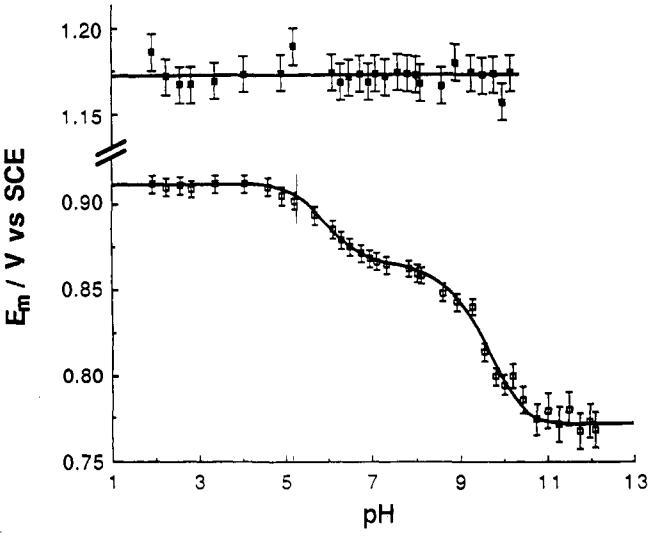

Figure 2. Nernst–Clark plots of (**1**)$Fe(X)_2$ midpoint oxidation potential vs pH determined at 0.20 V/s with a 7-μm carbon microelectrode. Solid lines represent theoretical fits to the experimental points: bottom (□), first 1e⁻ oxidation of (**1**)$Fe^{III}(X)_2$ and top (■); 1e⁻ oxidation of (**1**)-$Fe^{IV}(X)_2$.

Results

The pH dependence of the electrochemical reduction and oxidation, in water, of the hydrates of 5,10,15,20-tetrakis(2,6-dimethyl-3-sulfonatophenyl)porphinatoiron(III) ((**1**)$Fe^{III}(X)_2$ and -manganese(III) ((**1**)$Mn^{III}(X)_2$ (where X = H_2O or HO^-) have been examined in water (μ = 0.2, $NaNO_3$). The water-soluble metal(III) porphyrins used exist as one or more of three species (eq 2), dependent on pH. Because of the ortho methyl substituents, neither (**1**)$Fe^{III}(X)_2$ or (**1**)$Mn^{III}(X)_2$ form μ-oxo dimers. All potentials are vs SCE.[11]

$$(1)M^{III}(OH_2)_2 \overset{pK_{a1}}{\rightleftharpoons} (1)M^{III}(OH)(OH_2) + H^+$$

$$(1)M^{III}(OH)(OH_2) \overset{pK_{a2}}{\rightleftharpoons} (1)M^{III}(OH)_2 + H^+ \qquad (2)$$

The pH Dependence of the Potentials for Reduction and Oxidation of (1)$Fe^{III}(X)_2$ in Water Solvent (Ionic Strength 0.2 with

$NaNO_3$) Was Determined between pH 1.9 and 12.1. Scanning with a carbon microelectrode at 0.2 V/s, the midpoint potential of the first oxidation of (**1**)$Fe^{III}(X)_2$ shifts from 0.91 V below pH 5 to 0.77 V above pH 11 as shown in the bottom of Figure 1. A plot of E_m vs pH is shown in Figure 2. Three plateau regions are observed, one below pH 5, a smaller second plateau between pH 7 and 8, and a plateau above pH 11. Between pH 5 and 7 and pH 8 and 11 the midpoint potential decreases with a slope of ~ -0.06 V per pH unit. The midpoint potential of the second oxidation of (**1**)$Fe^{III}(X)_2$ [i.e., $1e^-$ oxidation of (**1**)$Fe^{IV}(X)_2$] is pH independent with a value of 1.17 V and can only be observed below pH 11 due to the intervention of the HO^- envelope at higher pH values.

Controlled-potential coulometry of (**1**)$Fe^{III}(X)_2$, at pHs 3.1, 5.2, 6.7, 7.2, 9.3, and 10.6, shows that the first oxidation is a one-electron process. Spectroelectrochemical observations during $1e^-$ oxidation of (**1**)$Fe^{III}(X)_2$ parallel observations recorded for the oxidation of (**1**)$Fe^{III}(X)_2$ by *tert*-butyl hydroperoxide.[12] Above pH 7, the electrochemically generated iron(IV) moiety has an absorption spectra nearly identical with that of a porphyrin moiety generated by the reaction of *t*-BuOOH with (**1**)$Fe^{III}(X)_2$ at the same pH (Soret band at 412 nm). Other similarities follow. Between pH 6 and 7 the electrochemically generated (**1**)$Fe^{IV}(X)_2$ exhibits a Soret band at 390 nm. The bathochromic shift of 24 nm is accompanied by a 10% drop in absorbance. After a lag phase, a new Soret begins to appear at 419 nm which reaches a maximum absorbance which is 90% that of (**1**)$Fe^{III}(X)_2$. Below pH 6, the Soret of (**1**)$Fe^{III}(X)_2$ and (**1**)$Fe^{IV}(X)_2$ are both at 392 nm with the excitation coefficient of (**1**)$Fe^{IV}(X)_2$ being 70% that of (**1**)$Fe^{III}(X)_2$.

Between pH 3 and 8, the halfwave potential for the one-electron reduction of (**1**)$Fe^{III}(X)_2$ at a 1-mm glassy carbon electrode varies from −0.28 to −0.59 V. Above pH 9.5 the halfwave potential is constant at −0.59 V. Electrochemical studies with a carbon-rotating ring-disk electrode, or a carbon microelectrode, show that equilibrium exists between two (**1**)$Fe^{III}(X)_2$ species. Below pH 6, the oxidation midpoint potential is observed at −0.28 V. At pH > 8, the midpoint potential has shifted to −0.55 V. However, between pH 6 and 8 two reductions are observed. At a carbon microelectrode the measured currents at both high (> pH 8) and low pH (< pH 6) correspond to a $1e^-$ reduction of (**1**)$Fe^{III}(X)_2$ within experimental error, as shown by comparison to the current measured for the oxidation of (**1**)$Fe^{III}(X)_2$. The sum of the currents for the two reductions observed between pH 6 and 8 is equal to a $1e^-$ reduction. As the pH is increased from 6 to 8 the current associated with the reduction at −0.28 decreases in magnitude, while that associated with the reduction at −0.55 increases. This explains (Discussion, Figure 3) the appearance of the upper plot of E_m vs pH for the $1e^-$ reduction of (**1**)$Fe^{III}(X)_2$.

The second reduction of (**1**)$Fe^{III}(X)_2$] i.e., $1e^-$ reduction of (**1**)$Fe^{II}(X)_2$] is pH independent (Figure 3) with a midpoint potential of −1.15 V.

The pH Dependence of the Potentials for Reduction and Oxidation of (1)$Mn^{III}(X)_2$ in Water Solvent (Ionic Strength 0.2 with $NaNO_3$) Was Determined between pH 1.3 and 10.8. Scanning with a carbon microelectrode at 0.5 V/s, the midpoint potential of the first oxidation of (**1**)$Mn^{III}(X)_2$ shifts from 1.04 V below pH 3 to 0.86 V at pH 10.8. A plot of E_m vs pH is shown in Figure 4. Two plateau regions are observed, one with a potential of 1.04 V between pH 1.3 (the lowest pH used) and pH 3 and a second plateau between pH 6.4 and 9.5 with a potential of 0.93 V. Between pH 3.5 and 6 and above pH 10 the midpoint potential decreases with a slope of ~ -0.06 V per pH unit.

The midpoint potential of the second oxidation of (**1**)$Mn^{III}(X)_2$ [i.e., $1e^-$ oxidation of (**1**)$Mn^{IV}(X)_2$] decreases from 1.21 V at pH 1.8 to 1.15 V at pH 9. Two plateau regions are observed, one with a potential of 1.21 V between pH 1.8 and 2.8, and a second between pH 5.3 and 9 with a potential of 1.15 V. The second $1e^-$ oxidation of (**1**)$Mn^{III}(X)_2$ can only be observed above pH 1.8 and below pH 10. Spectroelectrochemical results, below pH 1.8, indicate that the second oxidation causes demetalation of (**1**)-

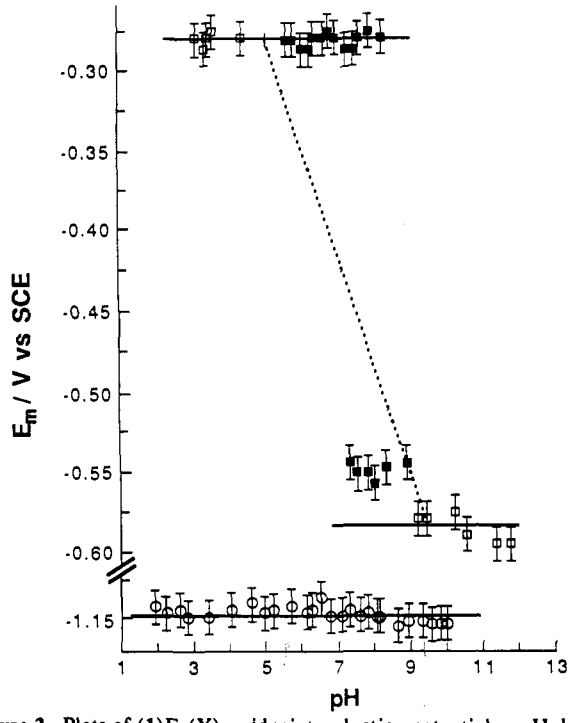

Figure 3. Plots of (**1**)$Fe(X)_2$ midpoint reduction potential vs pH determined at 0.010 V/s with a 7-μm carbon microelectrode. Solid lines represent Nernst–Clark theoretical fits to the experimental points: top (□, ■), $1e^-$ reduction of (**1**)$Fe^{III}(X)_2$. The closed box represents the region in which two midpoint potentials are simultaneously observed for the $1e^-$ reduction of (**1**)$Fe^{III}(X)_2$: bottom (○), $1e^-$ reduction of (**1**)-$Fe^{II}(X)_2$.

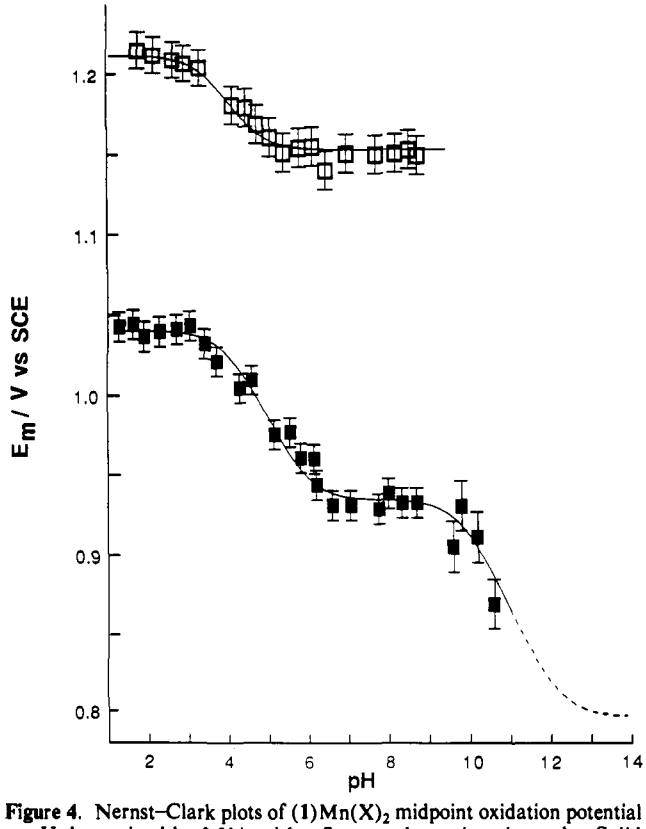

Figure 4. Nernst–Clark plots of (**1**)$Mn(X)_2$ midpoint oxidation potential vs pH determined by 2 V/s with a 7-μm carbon microelectrode: Solid lines represent theoretical fits to the experimental points: bottom (■), $1e^-$ oxidation of (**1**)$Mn^{III}(X)_2$ and top (□), $1e^-$ oxidation of (**1**)$Mn^{IV}(X)_2$.

(11) Gopinath, E.; Bruice, T. C., following paper in this issue.
(12) Balasubramanian, P. N.; Smith, J. R. L.; Davis, M. J.; Kaaret, T. W.; Bruice, T. C. *J. Am. Chem. Soc.* **1989**, *111*, 1477.

Table I. Acid Dissociation Constants, Calculated from the Nernst–Clark Plots of Figures 2 and 3, for Water Species Ligated to the Various Oxidation States of Iron 5,10,15,20-Tetrakis(2,6-dimethyl-3-sulfonatophenyl)porphyrin

species	pK_{a1}	pK_{a2}
$(1)Fe^{II}(X)$	9.7 ± 0.7[a]	*b*
$(1)Fe^{III}(X)_2$	6.55 ± 0.15	10.55 ± 0.2
$(1)Fe^{IV}(X)_2$	5.7 ± 0.15	9.0 ± 0.2
$(^{\bullet+}1)Fe^{IV}(X)_2$	5.7 ± 0.15[c]	9.0 ± 0.2[c]

[a] This is not a defined pK_a value but a position of a break in the Nernst–Clark plot. Though, Nernst–Clark equations are not applicable to a system which is not at thermodynamic equilibrium, such a pK_a value is not unreasonable. [b] Not observed. [c] Acid dissociation constants of $(^{\bullet+}1)Fe^{IV}(X)_2$ are identical with those of $(1)Fe^{IV}(X)_2$; see text.

$Mn^{III}(X)_2$. At high pH, intervention of the HO^- envelope interferes with the determination of the midpoint potential.

Discussion

The pH dependence of the oxidation and reduction potentials of the hydrates of 5,10,15,20-tetrakis(2,6-dimethyl-3-sulfonatophenyl)porphinatoiron(III) $\{(1)Fe^{III}(X)_2\}$ and -manganese(III) $\{(1)Mn^{III}(X)_2\}$ (X = H_2O, HO^-, or the oxo ligand O^{2-}) have been investigated in water as a function of pH at an ionic strength of 0.2 (with $NaNO_3$).

Electrochemistry of $(1)Fe(X)_2$. The electrochemistry of $(1)Fe^{III}(X)_2$ is dependent upon pH due to the equilibria of Scheme I. The dependence of midpoint potential upon pH is shown in Figure 2. The lines generated to fit the experimental points were obtained by computer fitting of the appropriate Nernst–Clark equation (Scheme II) which was derived by use of the equilibria in Scheme I.[13]

Scheme I

$$(1)Fe^{II}(H_2O) \overset{K_{a1}^{II}}{\rightleftharpoons} (1)Fe^{II}(OH)$$

$$(1)Fe^{III}(H_2O)_2 \overset{K_{a1}^{III}}{\rightleftharpoons} (1)Fe^{III}(H_2O)(OH) \overset{K_{a2}^{III}}{\rightleftharpoons} (1)Fe^{III}(OH)_2$$

$$(1)Fe^{IV}(H_2O)_2 \overset{K_{a1}^{IV}}{\rightleftharpoons} (1)Fe^{IV}(H_2O)(OH) \overset{K_{a2}^{IV}}{\rightleftharpoons} (1)Fe^{IV}(OH)_2$$

$$(1^{\bullet+})Fe^{IV}(H_2O)_2 \overset{K_{a1}^{V}}{\rightleftharpoons} (1^{\bullet+})Fe^{IV}(H_2O)(OH) \overset{K_{a2}^{V}}{\rightleftharpoons} (1^{\bullet+})Fe^{IV}(OH)_2$$

Shown in Table I are the acid dissociation constants for $(1)Fe^{III}(X)_2$, $(1)Fe^{IV}(X)_2$, and $(1^{\bullet+})Fe^{IV}(X)_2$, obtained from the best fit of the appropriate Nernst–Clark equation to the experimental points. The pK_{a1}^{II} for $(1)Fe^{II}(X)_2$ could not accurately be determined. Microelectrode and rotating ring results indicate that the reduction $(1)Fe^{III}(X)_2$ to $(1)Fe^{II}(X)_2$ does not come to a thermodynamic equilibrium within the time scale of the electrochemical experiments used. The nonequilibrium is mostly due to the loss of a ligand when an iron(III) porphyrin is reduced to an iron(II) porphyrin.

The electrochemically measured pK_{a1}^{III} of 6.55 for $(1)Fe^{III}(X)_2$ compares favorably to that determined by spectrophotometric titration (6.75) at an ionic strength of 0.2.[14] The second acid dissociation constant, K_{a2}^{III} cannot be observed by spectrophotometric titration because of the close similarity in the spectra of $(1)Fe^{III}(OH)(H_2O)$ and $(1)Fe^{III}(OH)_2$. The pK_{a2}^{III} value of 10.55 (range 10.45–10.65) is close to a pK_a (10.9) required to fit the log second-order rate constant vs pH plot for the reaction of $(1)Fe^{III}(X)_2$ with *tert*-butyl hydroperoxide.[11]

The dependence upon iron oxidation state of first pK_a values (Table I) is predictable. In going from $(1)Fe^{II}(X)_2$ to $(1)Fe^{IV}(X)_2$ the iron moiety is made more electropositive such that the electron density of the ligated water and its pK_a are decreased. Absence of a pH dependence in the oxidation of $(1)Fe^{IV}(X)_2$ to $(1^{\bullet+})Fe^{IV}(X)_2$ indicates that any pK_a values of the iron(IV) porphyrin and iron(VI) porphyrin π-cation radical species must be nearly the same. Our electrochemical observations support the findings[15] that a 2e oxidation of an oxo-ligated iron(III) porphyrin provides an iron(IV) porphyrin π-cation radical rather than an iron(V) porphyrin. Formation of an iron(V) porphyrin would lower the pK_as of ligated H_2O relative to that of the iron(IV) porphyrin due to (i) the increased electropositivity of the iron and (ii) the driving force to reach electroneutrality in the iron moiety.

(13) Clark, W. M. *Oxidation–Reduction Potentials of Organic Systems*; R. E. Krieger: Huntington, NY, 1972, Chapter 4.

(14) The first pK_a of $(1)Fe^{III}(X)_2$ is dependant upon solution ionic strength; see the following paper in this issue for more details.

Table II. Acid Dissociation Constants, Calculated from the Nernst–Clark Plots of Figure 4, for Water Species Ligated to the Various Oxidation States of Manganese 5,10,15,20-Tetrakis(2,6-dimethyl-3-sulfonatophenyl)porphyrin

species	pK_{a1}	pK_{a2}
$(1)Mn^{III}(X)_2$	5.8 ± 0.4	12.2 ± 0.05[a]
$(1)Mn^{IV}(X)_2$	4.1 ± 0.4[b]	9.9 ± 0.6[b]
	4.7 ± 0.4[c]	*d*
$(1)Mn^{V}(X)_2$	3.7 ± 0.4[c]	*d*

[a] Measured spectrophotometrically, from ref 5. [b] Determined from the $1e^-$ oxidation of $(1)Mn^{III}(X)_2$. [c] Determined from the $1e^-$ oxidation of $(1)Mn^{IV}(X)_2$. [d] Not observed.

The midpoint potentials at the three pH independent regions in the plot of E_m vs pH for $1e^-$ oxidation of $(1)Fe^{III}(X)_2$ can be thought of as apparent formal potentials ($E^{\circ\prime}$) as shown in eqs 3–5. If we assume, below pH 5, that $(1)Fe^{III}(X)_2$ is present as $(1)Fe^{III}(H_2O)_2$ (eq 3),[16] then between pH 7 and 8 it is present

$$(1)Fe^{IV}(H_2O)_2 + e^- \rightleftharpoons (1)Fe^{III}(H_2O)_2 \qquad E^{\circ\prime} = 0.91 \pm 0.01\ V \tag{3}$$

$$(1)Fe^{IV}(H_2O)(OH) + e^- \rightleftharpoons (1)\ Fe^{III}(H_2O)(OH) \qquad E^{\circ\prime} = 0.86 \pm 0.03\ V \tag{4}$$

$$(1)Fe^{IV}(OH)_2 + e^- \rightleftharpoons (1)Fe^{III}(OH)_2 \qquad E^{\circ\prime} = 0.77 \pm 0.05\ V \tag{5}$$

as $(1)Fe^{III}(H_2O)(OH)$ (eq 4) and as $(1)Fe^{III}(OH)_2$ above pH 11 (eq 5). In separate experiments E_m values for reduction of iron(IV) to iron(III) porphyrin species were carried out in D_2O. From comparison of plots of E_m vs pH (in H_2O) to E_m vs pD (in D_2O) the $E^{\circ\prime}$ values of eqs 3, 4, and 5 do not, within experimental error, exhibit deuterium solvent isotope effects. The deuterium solvent isotope effects for acid dissociation constants (K_a^H/K_a^D) are 5.0 for K_{a1}^{III}, 2.5 for K_{a2}^{III}, 7.9 for K_{a1}^{IV}, and 3.5 for K_{a2}^{IV}.

Scheme II

For the $1e^-$ oxidation of $(1)Fe^{III}(X)_2$

$$E_m = E'_o + \frac{RT}{F} \ln \left[\frac{(a_H)^2 + K_{a1}^{III} a_H + K_{a1}^{III} K_{a2}^{III}}{(a_H)^2 + K_{a1}^{IV} a_H + K_{a1}^{IV} K_{a2}^{IV}} \right] \tag{a}$$

For the $1e^-$ oxidation of $(1)Fe^{IV}(X)_2$

$$E_m = E'_0 + \frac{RT}{F} \ln \left[\frac{(a_H)^2 + K_{a1}^{IV} a_H + K_{a1}^{IV} K_{a2}^{IV}}{(a_H)^2 + K_{a1}^{V} a_H + K_{a1}^{V} K_{a2}^{V}} \right] \tag{b}$$

For the $1e^-$ reduction of $(1)Fe^{III}(X)_2$

$$E_m = E'_o + \frac{RT}{F} \ln \left[\frac{a_H + K_{a1}^{II}}{(a_H)^2 + K_{a1}^{III} a_H + K_{a1}^{III} K_{a2}^{III}} \right] \tag{c}$$

Electrochemistry of $(1)Mn(X_2)$ in Water Solvent (Ionic Strength 0.2 with $NaNO_3$). The dependence of the electrochemistry of

(15) Groves, J. T.; Haushalter, R. C.; Nakamura, M.; Nemo, T. E.; Evans, B. J. *J. Am. Chem. Soc.* **1981**, *103*, 2884.

(16) Because of the occurrence of two acid dissociation constants for $(1)Fe^{III}(X)_2$ the species present at pHs below the first pK_a must be a species which can lose two protons. From the choices $(1)Fe^{III}(H_2O)_2$, $(1)Fe^{III}(H_3O^+)(H_2O)$, $(1)Fe^{III}(H_3O^+)_2$, $(1)Fe^{III}(H_2O)(O)$, $(1)Fe^{III}(OH)_2$; or $(1)Fe^{III}(H_2O)(OH)$ only the first can provide chemically reasonable deprotonated structures for all pHs and oxidation states.

(1)$Mn^{III}(X)_2$ upon pH can be discussed in terms of the equilibria provided in Scheme II for (1)$Fe^{III}(X)_2$. Dependence of midpoint potentials upon pH is shown in Figure 4. The lines generated to fit the points were obtained by computer fitting of the appropriate Nernst–Clark equation (similar to that shown for (1)$Fe(X)_2$ in Schemes I and II). In Table II are the acid dissociation constants for (1)$Mn^{III}(X)_2$, (1)$Mn^{IV}(X)_2$, and (1)$Mn^{V}(X)_2$ [or ($1^{\bullet+}$)$Mn^{IV}(X)_2$] which were obtained from the best fit of the appropriate Nernst–Clark equation to the measured midpoint potentials.

The pK_a values for (1)$Mn^{IV}(X)_2$ in Table II were determined from both the $1e^-$ oxidation of (1)$Mn^{III}(X)_2$ and (1)$M^{IV}(X)_2$. The pK_a values determined from the $1e^-$ oxidation of (1)$Mn^{IV}(H_2O)_2$ are 0.2 and 0.5 pH units higher than those determined from the $1e^-$ oxidation of (1)$Mn^{III}(X)_2$. The probable explanation for this discrepancy is that the potential for $1e^-$ oxidation of (1)$Mn^{IV}(X)_2$ species approaches that for the oxidation of HO^-. Therefore, in the $1e^-$ oxidation of (1)$Mn^{IV}(X)_2$ in unbuffered medium, the pH at the surface of the electrode is lower than that in the bulk of the solution. Therefore, the better pK_a values are those determined from the $1e^-$ oxidation of (1)$Mn^{III}(X)_2$. Also using the same logic, the pK_a value of (1)$Mn^{V}(H_2O)_2$ is most likely ~0.4 pH units lower than shown in Table II.

The apparent formal potentials ($E^{\circ\prime}$) for (1)$Mn^{III}(X)_2$/(1)$Mn^{IV}(X)_2$ redox couple are shown in eqs 6, 7, and 8. If we assume, below pH 3, that (1)$Mn^{III}(X)_2$ is present as (1)$Mn^{III}(H_2O)_2$, then between pH 6.4 and 9.5 it must be present as (1)$Mn^{III}(H_2O)(OH)$ and above pH 12.7 as (1)$Mn^{III}(OH_2)_2$. The apparent formal potential of (1)$Mn^{III}(OH)_2$ was estimated from the Nernst–Clark equations by using the spectrophotometrically determined pK_a of 12.2.[5]

$$(1)Mn^{IV}(H_2O)_2 + e^- \rightleftharpoons (1)Mn^{III}(H_2O)_2$$
$$E^{\circ\prime} = 1.04 \pm 0.01 \text{ V} \quad (6)$$

$$(1)Mn^{IV}(H_2O)(OH) + e^- \rightleftharpoons (1)Mn^{III}(H_2O)(OH)$$
$$E^{\circ\prime} = 0.93 \pm 0.02 \text{ V} \quad (7)$$

$$(1)Mn^{IV}(OH)_2 + e^- \rightleftharpoons (1)Mn^{III}(OH)_2$$
$$E^{\circ\prime} = 0.7 \pm 0.1 \text{ V} \quad (8)$$

The decrease in the first pK_as with increase in the oxidation state of manganese (for Mn(III) and Mn(IV) is qualitatively the same as observed for the (1)$Fe(X)_2$ system. Presence of a pH dependence in the oxidation of (1)$Mn^{IV}(X)_2$ to (1)$Mn^{V}(X)_2$ [or ($1^{\bullet+}$)$Mn^{IV}(X)_2$] indicates that the product of the $1e^-$ oxidation of (1)$Mn^{IV}(X)_2$ can more accurately be described as a manganese(V) porphyrin. Expectation would be that the formation of a manganese(IV) porphyrin π-cation radical would have little effect on the pK_a, whereas formation of a manganese(V) porphyrin would lower the pK_as relative to that of manganese(IV) porphyrin due to (1) the increase electropositivity of the manganese and (2) the driving force to reach electroneutrality in the manganese.

Of considerable importance in the finding that with water as solvent H_2O and HO^- are the axial ligands of $[(porph)M]^{2+}$ and $[(porph)M]^{3+}$ species such that oxo ligation cannot be important except at high pH [where the proton inventory of structures such as ($1^{\bullet+}$)$Fe^{IV}(OH)_2$ and ($1^{\bullet+}$)$Fe^{IV}(=O)(H_2O)$ are the same.]

Acknowledgment. This study was supported by a grant from the National Institutes of Health.